

(Supporting material)

Tuning membrane phase separation using non-lipid amphiphiles

Hari S. Muddana¹, Homer H. Chiang¹, and Peter J. Butler^{1*}

¹Department of Bioengineering, Pennsylvania State University, 205 Hallowell Building, University Park, PA 16803

S.I. Atomistic simulations

Molecular topologies of vitamin-E (VE), triton-X (TX), and benzyl alcohol (BA) were constructed using DUNDEE PRODRG server.¹ The united atom model was adopted for CH_n groups. Force field parameters for lipids were identical to Berger et al.² and force field parameters for VE, TX, and BA were adopted from GROMOS 45a4 set.³ Partial charges of DPPC were obtained from Chiu et al.,⁴ whereas partial charges for VE, TX, and BA were assigned according to GROMOS force field.³ Simple point charge (SPC) model was used for the explicit water molecules.

A simulation box of 1,2-dipalmitoyl-sn-glycero-3-phosphocholine (DPPC) bilayer consisting of 128 DPPC molecules (64 in each leaflet) and 3655 water molecules was obtained from Tieleman et al.⁵ Simulations were carried out on four different systems: pure bilayer (control), and bilayers with VE (6 in each leaflet), TX (6 in each leaflet), and BA (100 in each leaflet). VE/TX/BA molecules were placed in the water phase at random locations on both sides of the lipid bilayer, and allowed to freely intercalate into the membrane. Once all amphiphilic molecules penetrated the membrane, the resulting concentrations were approximately 10 mol% VE, 10 mol% TX, and 60 mol% BA as calculated from mol % = moles of amphiphiles / (moles of amphiphiles + lipids). Molecular dynamics simulations were carried out using GROMACS simulation software (version 4.0.3).^{6,7} Starting simulation structures were energy minimized using steepest-descent algorithm for at least 1000 steps and further equilibrated under NPT conditions for 1ns, with temperature and pressure set to 323 K and 1 bar, respectively. Final production runs were carried out under NPT conditions with temperature and pressure set to 323 K and 1 bar, respectively. Periodic boundary conditions were applied to the simulation box in all three coordinate dimensions (with x, y in the bilayer plane and z normal to the bilayer). Temperature and pressure of the system were controlled using Berendsen's weak coupling method with the time constants set to 0.1 ps and 1.0 ps respectively.⁸ Semi-anisotropic scaling

was used for pressure coupling, with 1 bar reference pressure in the xy plane and z-dimension. The LINCS algorithm was used to constrain bond lengths.^{6,7} The Particle-Mesh Ewald (PME) method was used for electrostatic interactions, with a direct-space cutoff of 1nm, and cubic interpolation for the calculation of long-range interactions in the reciprocal space, with a Fourier transform grid of 0.12 nm maximum.⁹ The Lennard-Jones interactions were cutoff at 1.0 nm. A time-step of 2 fs was used with a leap-frog integration algorithm for the equations of motion.⁷ Initially all the systems were equilibrated until the area-per-lipid stabilized, to ensure complete intercalation of the additives. Final production runs were carried out for a total simulation time of 20 ns.

S.II. Coarse-grained simulations

The MARTINI model was used in all coarse-grained simulations. MARTINI parameters for various lipids, sterols, and small molecules are available at <http://md.chem.rug.nl/cgmartini/index.php/home>. Atomistic to coarse-grained (CG) mappings for VE, TX, and BA are shown in Figure S1. CG parameters for the VE headgroup beads were assigned in accord with the model for cholesterol; with the exception that the bead with ester oxygen was assigned intermediate polarity. Parameters for VE tail beads were assigned based on butane (C1) for groups with four carbons and propane (C2) for groups with three carbons. Headgroup of TX was assigned parameters based on butane (C1) and benzene (SC1), whereas tail group beads were assigned SNa type with intermediate polarity and hydrogen bond accepting ability. The terminal tail bead of Triton-X was assigned the parameters of SNda, with both hydrogen bond donating and accepting ability. Bead types for benzyl alcohol were assigned based on benzene (SC4) and ethanol (P2). Bond lengths and bond angles between CG bead types were determined from the atomistic simulations. Default force constant of 1250 kJ/mol.nm² and 25 kJ/mol.rad² were used for bonds and angles, respectively.

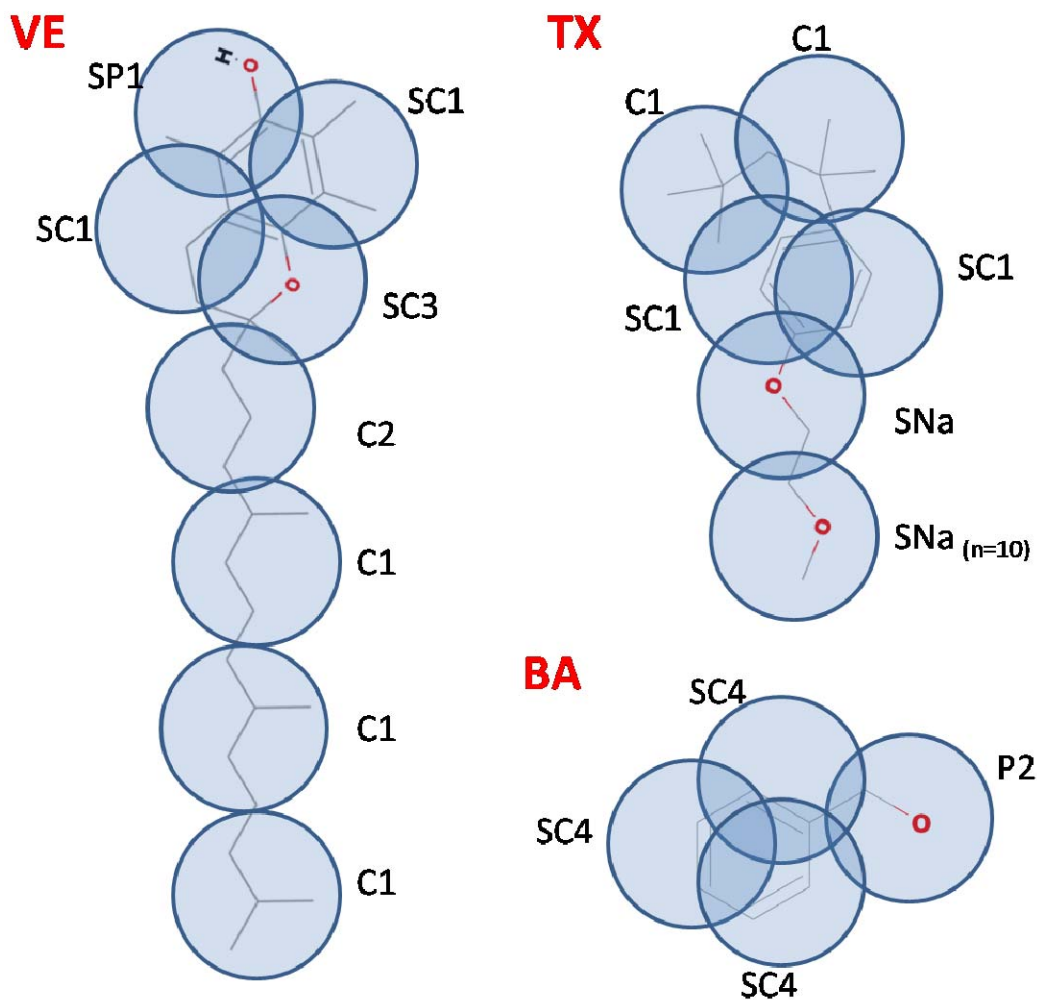


Figure S1. Coarse-grained mapping of VE, TX, and BA.

Simulation protocol. Periodic boundary conditions were applied in all three coordinate dimensions (with x,y in the bilayer plane and z normal to the bilayer). Temperature and pressure of the system were controlled using Berendsen's weak coupling method with the time constants set to 0.4 ps and 4.0 ps respectively. Semi-anisotropic scaling was used for pressure coupling, with 1 bar reference pressure in the xy plane and z-dimension. Electrostatic and Lennard-Jones interactions were smoothly switched off at 1.2 nm. A time step between 15 and 30 fs, depending on the stability of the simulations, was used with leap-frog integration for integrating the equations of motion. Final production runs were carried out for a total simulation time of at least 600 ns, which corresponds to an effective simulation time of 2.4 μ s. Data analysis was performed on the last 200 ns (simulation time) of the trajectory. Initially, a small simulation box was prepared consisting of 64 1,2-dipalmitoyl-sn-glycero-3-phosphocholine (DPPC) molecules and 64 1,2-dilinoleoyl-sn-glycero-3-phosphocholine (DUPC) molecules, with 32 of each in each

leaflet. 6 CG waters per lipid were added to the simulation box. The entire system was first energy minimized using steepest-descent algorithm and then equilibrated under NPT conditions for 200 ns, with temperature and pressure set to 300 K and 1 bar, respectively. A larger system consisting of 2048 lipids and 12888 CG waters was constructed by replicating the smaller equilibrated system along the x- and y-dimensions four times. Simulations were carried out on four different systems: pure bilayer (control), and bilayers with VE (10 mol %), TX (10 mol %), and BA (60 mol %). VE/TX/BA molecules were initially placed in the water phase at random locations on both sides of the lipid bilayer, and allowed to freely intercalate into the membrane. All the systems were equilibrated until the additive molecules intercalated into the membrane and the area-per-lipid was stabilized.

S.III. Validation of coarse-grained parameters

Coarse-grained parameters for VE, TX, and BA were validated by comparing the location and distribution of the additives across the membrane-water interface with those obtained from atomistic simulations. We computed the mass density profiles of the different chemical groups of additives along the direction of membrane normal, shown in figure S2. In addition to the effect of coarse-graining, membrane undulations exhibited in CG simulations also contribute to the smoothing of the mass-density profiles. Nevertheless, the peaks observed in the density profiles are good indicators for the relative positioning of different chemical groups of the additives along the membrane interface.

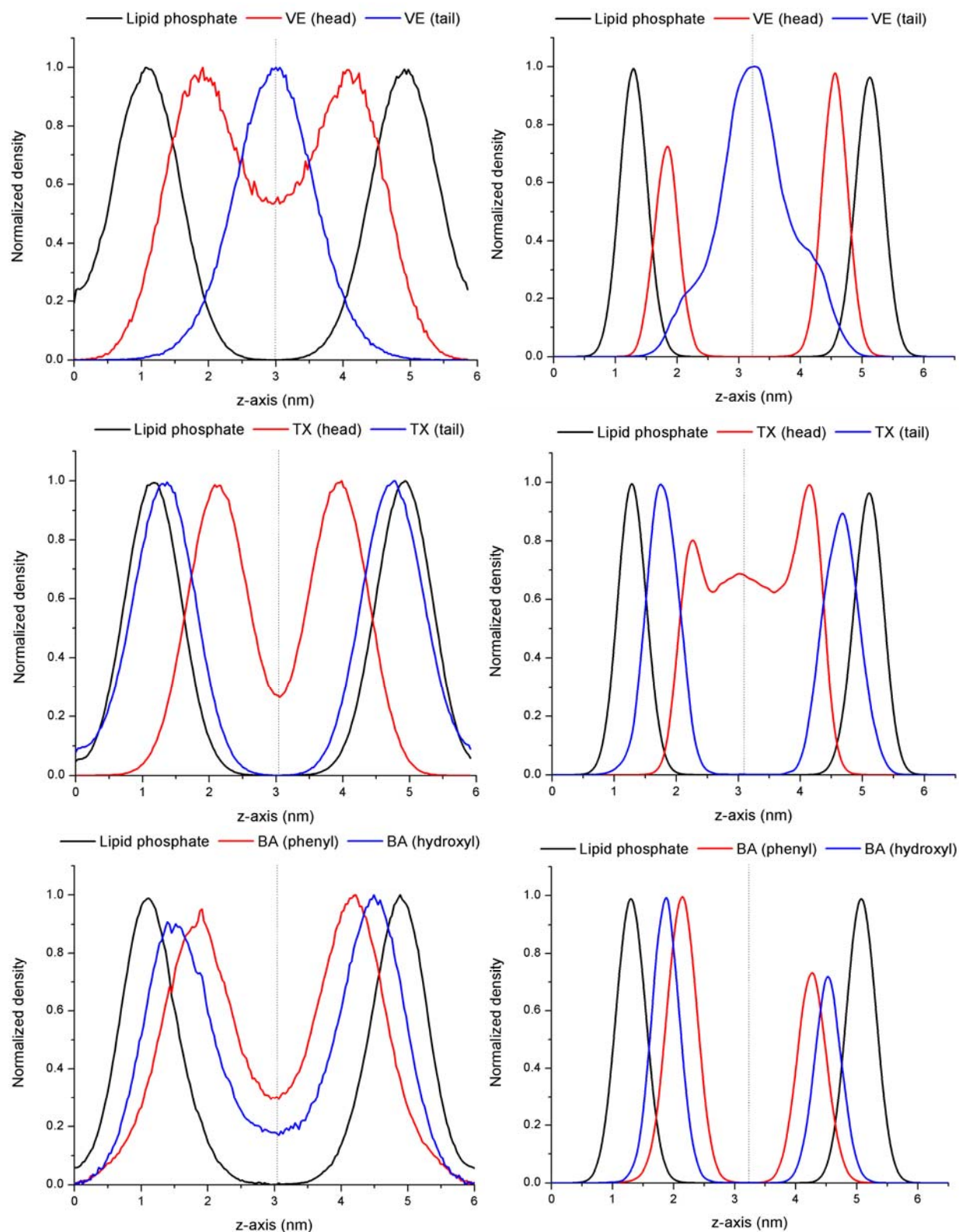


Figure S2. Normalized mass-density profiles of lipid phosphate group and additives (top - vitamin-E, middle - Triton-X, bottom - benzyl alcohol) along membrane normal, computed from coarse-grained simulations (left) and atomistic simulations (right). Center of the bilayer is indicated by a dotted line.

In atomistic simulations, we observed that the hydroxyl group of both benzyl alcohol and triton-X were located at the lipid headgroup region predominantly hydrogen bonded to the phosphate or ester oxygen atoms. The ethylene oxide chain of triton-X adopted a partially extended conformation and was located at the lipid-water interface, while its bulky hydrophobic group penetrated the lipid bilayer core. Unlike triton-X and benzyl alcohol, vitamin-E has a long hydrophobic tail region, and so adopted a linear conformation along the membrane normal. The terminal methylene groups were located at the bilayer mid-plane and the chromanol moiety was positioned below the lipid phosphates predominantly hydrogen bonded to the lipid acyl ester oxygen atoms. While specific atomic-level interactions such as hydrogen bonding cannot be directly observed in coarse-grained simulations, the relative positioning of the different chemical groups of the additives along the membrane interface were consistent with those observed in atomistic simulations, as shown in figure S2.

We further compared the changes in chain order parameter under the influence of different additives. Order parameters computed from the coarse-grained simulations are shown in figure 4 of main text. Order parameters from atomistic simulations were computed as an average of both acyl chains under different simulation conditions, as described previously¹⁰ (shown in figure S3). Incorporation of vitamin-E in the bilayer caused a significant increase in the order of the acyl chains, uniformly throughout the length of the carbon chain. This result can be explained by the alignment of the vitamin-E molecule with the lipid acyl chains. This result is also consistent with electron spin resonance data where ordering in the fluid-phase bilayer increased upon incorporation of vitamin-E.^{11,12} Similarly, Triton-X also induced a significant increase in the chain order near the headgroup region. On the other hand, benzyl alcohol induced an increase in order near the headgroup region and a decrease in order near the tail region. The close proximity of the bulky hydrophobic moieties (benzyl group) to the lipid headgroup region orders the lipid acyl chains in this region. The decrease in acyl chain ordering in the tail regions is likely due to the increase in the overall tilt of the lipid chains. In general, these results from atomistic simulations are in good agreement with coarse-grained simulations. Increase in chain order of the fluid-phase (DUPC phase) was observed with both Triton-X and Vitamin-E, whereas a significant decrease in chain order was observed with benzyl alcohol. However, changes in the order parameter observed in coarse-grained simulation were uniform throughout the length of the lipid chains. This is likely due to the smoothing effect caused by coarse-graining the underlying

atomic motions. In summary, the effect of each of the additives on lipid chain order is qualitatively consistent between atomistic and coarse-grained simulations.

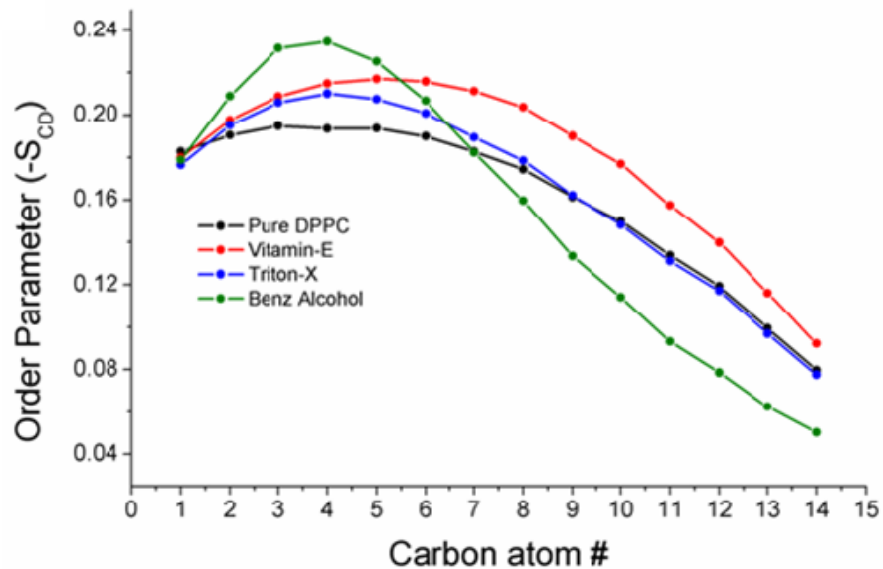


Figure S3. Chain order parameters of the lipids, averaged over both the chains, in pure bilayer (black), with vitamin-E (red), triton-X (blue), and benzyl alcohol (green).

S.IV. Additional Figures

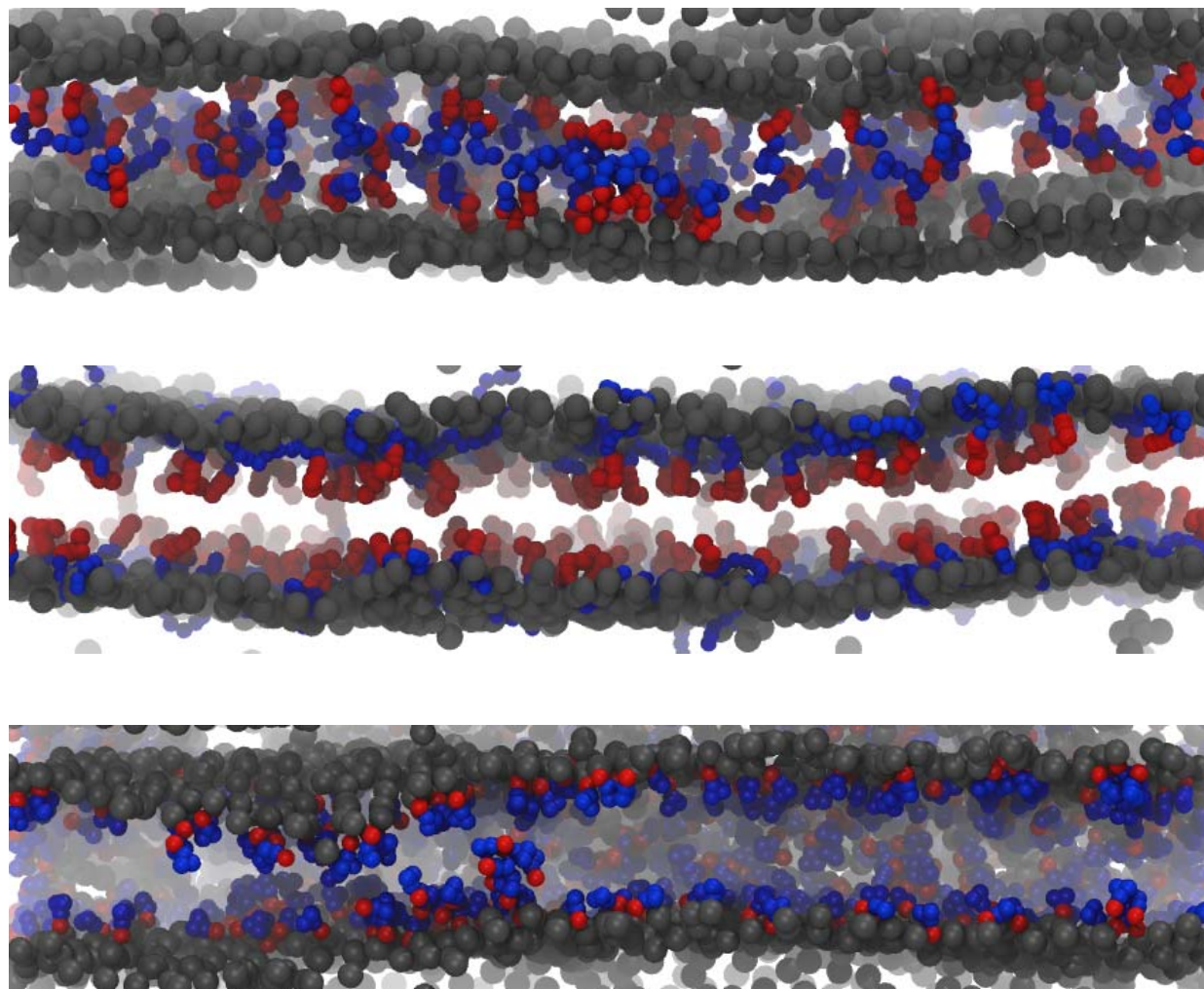


Figure S4. Side-view snapshots of the lipid bilayer with different additives, vitamin-E (top), triton-X (middle), and benzyl alcohol (bottom). Color legend: grey - lipid phosphate groups, red – additive headgroup, blue – additive tail group.

References

1. Schuttelkopf, A. W. and D. M. F. van Aalten. 2004. PRODRG: a tool for high-throughput crystallography of protein-ligand complexes. *Acta Crystallographica Section D-Biological Crystallography* 60:1355-1363.
2. Berger, O., O. Edholm, and F. Jahnig. 1997. Molecular dynamics simulations of a fluid bilayer of dipalmitoylphosphatidylcholine at full hydration, constant pressure, and constant temperature. *Biophysical Journal* 72:2002-2013.
3. Lins, R. D. and P. H. Hunenberger. 2005. A new GROMOS force field for hexopyranose-based carbohydrates. *Journal of Computational Chemistry* 26:1400-1412.
4. Chiu, S. W., M. Clark, V. Balaji, S. Subramaniam, H. L. Scott, and E. Jakobsson. 1995. Incorporation of Surface-Tension Into Molecular-Dynamics Simulation of An Interface - A Fluid-Phase Lipid Bilayer-Membrane. *Biophysical Journal* 69:1230-1245.
5. Tieleman, D. P. and H. J. C. Berendsen. 1996. Molecular dynamics simulations of a fully hydrated dipalmitoyl phosphatidylcholine bilayer with different macroscopic boundary conditions and parameters. *Journal of Chemical Physics* 105:4871-4880.
6. van der Spoel, D., E. Lindahl, B. Hess, G. Groenhof, A. E. Mark, and H. J. C. Berendsen. 2005. GROMACS: Fast, flexible, and free. *Journal of Computational Chemistry* 26:1701-1718.
7. Lindahl, E., B. Hess, and D. van der Spoel. 2001. GROMACS 3.0: a package for molecular simulation and trajectory analysis. *Journal of Molecular Modeling* 7:306-317.
8. Berendsen, H. J. C., J. P. M. Postma, W. F. Vangunsteren, A. Dinola, and J. R. Haak. 1984. Molecular-Dynamics with Coupling to An External Bath. *Journal of Chemical Physics* 81:3684-3690.
9. Essmann, U., L. Perera, M. L. Berkowitz, T. Darden, H. Lee, and L. G. Pedersen. 1995. A Smooth Particle Mesh Ewald Method. *Journal of Chemical Physics* 103:8577-8593.
10. Gullapalli, R. R., M. C. Demirel, and P. J. Butler. 2008. Molecular dynamics simulations of DiI-C-18(3) in a DPPC lipid bilayer. *Physical Chemistry Chemical Physics* 10:3548-3560.
11. Severcan, F. and S. Cannistraro. 1990. A Spin Label ESR and Saturation Transfer ESR Study of Alpha-Tocopherol Containing Model Membranes. *Chemistry and Physics of Lipids* 53:17-26.
12. Suzuki, Y., M. Tsuchiya, S. R. Wassall, Y. M. Choo, G. Govil, V. E. Kagan, and L. Packer. 1993. Structural and Dynamic Membrane-Properties of Alpha-Tocopherol and Alpha-

Tocotrienol - Implication to the Molecular Mechanism of Their Antioxidant Potency.
Biochemistry 32:10692-10699.